Steel and Composite Structures, *Vol. 28, No. 4 (2018) 403-414*
DOI: https://doi.org/10.12989/scs.2018.28.4.403

Lateral-torsional buckling of functionally graded tapered I-beams considering lateral bracing

Mohammad Rezaiee-Pajand [*], Amir R. Masoodi [a] and Ali Alepaighambar [b]

Department of Civil Engineering, Ferdowsi University of Mashhad, Mashhad, Iran

(*Received June 3, 2017, Revised April 7, 2018, Accepted June 4, 2018*)

Abstract. In this paper, the lateral-torsional buckling of axially-transversally functionally graded tapered beam is investigated. The structure cross-section is assumed to be symmetric I-section, and it is continuously laterally supported by torsional springs through the length. In addition, the height of cross-section varies linearly throughout the length of structure. The proposed formulation is obtained for the case that the elastic and shear modulus change as a power function along the beam length and section height. This structure carries two concentrated moments at the ends. In this study, the lateral displacement and twisting angle relation of the beam are defined by sinusoidal series. After establishing the eigenvalue equation of unknown constants, the beam critical bending moment is found. To validate the accuracy and correctness of results, several numerical examples are solved.

Keywords: functionally graded material; lateral and torsional buckling; tapered beam; warping; continuous torsional bracing

1. Introduction

In many structures, beam plays a practical and significant role. Since this part is rather thin, it should be kept safe from the stability phenomena. For this reason, many researchers have performed the stability analysis of the different beam under the various loading and boundary conditions. According to the findings, the axial tension-compression loads are effective on the bending stiffness of beams. On the other hand, these loadings increase or decrease the buckling load and unpaired bending vibrations. In the past years, many investigators studied the bending stability and vibration of the prismatic beams under the axial loads (Murthy and Neogy 1969, Gellert and Gluck 1972, Bokaian 1988, 1990, Leung 1991, Banerjee and Fisher 1992, Banerjee and Williams 1994, Hashemi *et al*. 1999, Hashemi and Richard 2000a, b, Jun *et al*. 2004). A few of these were performed on the combination effect of axial load and the ends bending moment on the stability and vibration of beam element (Joshi and Suryanarayan 1984, 1989, 1991, Pavlović and Kozić 2003, Pavlović *et al*. 2007).

Due to the needs, the structural elements can be modeled as a beam having complex geometric section. These parts can undergo the combination of axial, bending and torsional loadings. It is possible that the column having thin-walled section twists under the axial load. For this case, the buckling load of column should be determined based on the bending and torsional buckling simultaneously. Because of necessities, too many researchers have worked on the area of the bending-torsional buckling of beams and columns. For the same reason, some studies were performed on the effect of semi-rigid supports on the elastic bending or torsional and bending-torsional buckling of beams and columns. Among them, the works of (Winter 1958, Taylor and Ojalvo 1966, Nishino *et al*. 1973, Ioannidis *et al*. 1993, Valentino and Trahair 1998, Pi and Bradford 2002, Gupta *et al*. 2003, Andrade and Camotim 2004, Tsai and Kelly 2005) can be noted. Furthermore, the stability and vibration characteristics of three-dimensional steady motions of translating beams undergoing boundary misalignment were studied by Orloske and Parker (2006). In addition, a beam theory was suggested by Fatmi (2007) for the non-uniform warping analysis, including the effects of torsion and shear forces. On the other hand, the lateral buckling of a prismatic beam with homogenous section was studied based on the hyper-elastic formulation (Attard and Kim 2010). In another work, the torsional buckling of Chalipa section column, considering plastic deformation, was analyzed under the axial compression load (Schurig and Bertram 2011). Recently, a new and efficient warping displacement model was proposed to ensure the continuity of warping in beams with discontinuously varying arbitrary cross-sections (Yoon and Lee 2014).

In another research, the bending-torsional buckling of the steel beam with continuous lateral bracing was investigated (Larue *et al*. 2007). Moreover, a simple method was proposed to lateral-torsional analysis of doubly-symmetric I-beam considering continuous lateral bracing (Khelil and Larue 2008). On the other hand, the lateral-torsional buckling of I-beam having discrete lateral bracing was studied by Nguyen *et al*. (2010). Under the effect of the different loadings, the bending-torsional buckling strength

*Corresponding author, Professor,
E-mail: rezaiee@um.ac.ir
[a] Ph.D. Candidate
[b] Graduate Student

ISSN: 1229-9367 (Print), 1598-6233 (Online)

of I-beam with discrete supports was investigated (Nguyen *et al*. 2012). Furthermore, the ultimate strength of mono-symmetric I-beam was achieved by El-Mahdy and El-Saadawy (2015). Recently, the lateral-torsional strength of mono-symmetric I-beam having discrete lateral bracing was obtained (Mohammadi *et al*. 2016). However, none of the researches have studied the lateral-torsional buckling of tapered I-beam considering continuous and discrete lateral bracing. So far, the effect of functionally graded material, lateral bracing and the taper ratio of section on the lateral-torsional buckling of tapered I-beam was not studied simultaneously.

Due to some applications, investigating the effect of functionally graded materials in the static and dynamic buckling analysis of non-prismatic members is essential. In the past years, buckling analysis of non-prismatic members with FGM cross-section has rarely been studied. In 2001, the analysis of FGM beam was done by Sankar. The author assumed an exponential function for the modulus of elasticity variation throughout the height of the cross-section (Sankar 2001). In another work, an exact solution of free vibration and flexural analysis of the 2D beam on Winkler elastic foundation was proposed by Ying et al. in 2008. Exponential function was assumed for changing the modulus of elasticity (Ying *et al*. 2008). In 2011, buckling analysis of non-prismatic column with non-homogenous cross-section, which is affected by the axial joint load, was studied by Huang and Li (2011). In their study, for various columns, the governing differential equation for buckling of columns with varying flexural rigidity was reduced to a Fredholm integral equation. Flexural rigidity had a variety of functions, such as, polynomials, trigonometric and exponential functions (Huang and Li 2011). An analytical solution for buckling of prismatic Timoshenko and Euler-Bernoulli non-homogenous beam, which is affected by axial load, was found by Li and Batra (2013). Different boundary conditions were utilized by these investigators. Furthermore, the modulus of elasticity change in the height of the cross-section was assumed to be exponentially (Li and Batra 2013).

Recently, some studies were performed about the lateral-torsional buckling of tapered I-beam (Ioannidis and Avraam 2012, Michaltsos and Raftoyiannis 2012, Kim *et al*. 2013). An exact solution was proposed for the stability and free vibration analysis of thin-walled laminated beams (Kim and Lee 2014). In addition, the lateral-torsional buckling analysis of steel tapered I-beam was studied by (Kuś 2015). He assumed that the flange and web change along the length of the beam, simultaneously. On the other hand, the free vibration analysis of thin-walled composite I-beam was investigated by Vo *et al*. (2011). To analyze the behavior of FG beams under the effects of non-uniform torsion, a closed-form solution was proposed by Barretta *et al*. (2015). In order to achieve the optimum design, the analysis of flexural–torsional buckling of thin-walled composite beams was performed by Nguyen *et al*. (2015). On the other hand, the optimization of lateral buckling and free vibration of thin-walled laminated composite beams were analyzed by Nguyen *et al*. (2016). In their research, the section of the beam was assumed to be open-channel. In another work, nonlinear buckling analysis of thin-walled beams was performed by Lanc *et al*. (2016). They studied the effect of functionally graded material on the buckling behavior of the beam. It should be added that open cross-section beam was considered in their research. In another paper, a thin-walled beam formulation was presented for the dynamic analysis of bridges by Vieira *et al*. (2014). They considered warping effect in their formulation. Moreover, the design and construction of the Pre-Engineered Metal Building system in Korea were performed by Lee *et al*. (2015). They also evaluated the structural safety by using the finite element analysis program. Besides, a theoretical model and design procedure of thin-walled simply supported steel I-beams with an open cross section were incorporated by Aydin *et al*. (2015). They used energy method to obtain the buckling loads.

This article is devoted to the lateral-torsional buckling analysis of the tapered FG I-beam. In this study, the effect of concentrated moments at the two ends of the beam is considered. Moreover, the structural cross-section height changes linearly through the beam length. To develop the proposed formulation, the Euler-Bernoulli theory is employed. On the other hand, the variations of elastic and shear modulus along the height of section and length of the beam are defined as power functions. Furthermore, this structure is laterally braced throughout the length. To solve this problem, the sinusoidal series are utilized for the lateral-torsional deformations of beam section. After establishing total energy function, the eigenvalue equation of unknown constants is obtained. By utilizing this equation, the critical bending moment of the beam is calculated. Finally, some numerical examples are employed to validate the accuracy and correctness of suggested formulation.

2. Assumptions

Each analytical modeling has some assumptions. These are needed to achieve the solution of governing equations more easily. However, it is not allowable to ignore the factors having direct and intense effects on the results of analysis. The following assumptions are considered in this research:

(1) The shear deformation effect is neglected. Thus, the Euler-Bernoulli beam theory is considered in the proposed formulation. The base of the formulation is bending deformations and torsional rotations.
(2) The section of I-beam is doubly symmetric. In other words, the shear center is the same as the centroid.
(3) The large deformation effect is ignored in this paper. Therefore, the strains are assumed to be small.
(4) Two concentrated moments are applied at the two ends of beam element.
(5) The elastic and shear modulus change linearly along the length of the beam.
(6) The changes of elastic and shear modulus are formulated by a power function through the height of cross-section.
(7) dmIt should be added that cross-section keeps the main shape after the buckling.

3. Lateral-torsional buckling

Based on the previous researches, a beam element may lose its stability because of lateral-torsional buckling. In this failure mode, the buckling load of structure decreases, because its torsional stiffness is not adequate. It should be added that the traditional theory of the beam cannot consider both effects of the bending and torsion, simultaneously. Based on the energy method, the lateral-torsional analysis for this problem can be performed. To find the results, the total energy function should be minimized. In this study, the geometry of tapered I-beam and its cross-section, which is shown in Fig. 1, are utilized.

At this stage, the method of calculating torsion energy is presented. Fig. 1 shows the change of elastic modulus through the height of section. It should be added that the functions of changes of elastic and shear modulus are defined as follows

$$E(y)=E_f(x)\left(\left|\frac{y}{h}\right|+\frac{1}{2}\right)^n \qquad G(y)=G_f(x)\left(\left|\frac{y}{h}\right|+\frac{1}{2}\right)^n \tag{1}$$

$$\begin{aligned} E_f(x)&=E_{f,s}+(E_{f,L}-E_{f,s})\left(\frac{x}{L}\right)^2 \\ G_f(x)&=G_{f,s}+(G_{f,L}-G_{f,s})\left(\frac{x}{L}\right)^2 \end{aligned} \tag{2}$$

where the factor n is called the power constant. x is the longitudinal axis. On the other hand, the elastic modulus of start and end section of the beam are defined as $E_{f,s}$ and $E_{f,L}$, respectively. Furthermore, $G_{f,s}$ and $G_{f,L}$ are the shear modulus at the start and end section of structure. The parameter h is the height of section. In addition, the change of cross-section height through the length of the beam is estimated by the following function

$$h(x)=h_s+(h_L-h_s)\left(\frac{x}{L}\right) \tag{3}$$

in which h_s and h_L are used for the height of section at the start and end point of the beam. The length of the beam is defined by L. By including the boundary conditions of the simply supported beam, the twisting angle and lateral deformation functions can be estimated by sinusoidal series, such as below

$$\begin{aligned} w(x)&=\sum_{k=1}^{m+2} w_k \sin\left(\frac{k\pi x}{L}\right) \\ \phi(x)&=\sum_{k=1}^{m+2} \phi_k \sin\left(\frac{k\pi x}{L}\right) \end{aligned} \tag{4}$$

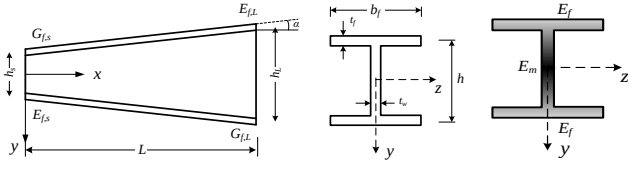

(a) Beam element (b) Cross-section (c) FGM

Fig. 1 The geometry of tapered FG I-beam

where w_k and ϕ_k are the general coordinates defined for the lateral deformation and torsioanl angle of the beam section, respectively. It is obvious that number of buckling modes considered for the element is equal to m+1. It should be noted that the boundary conditions are satisfied by the assumed functions.

3.1 Linear strain energy

The strain energy density function is defined by the symbol U_0. The total linear strain potential energy of the beam is expressed in the below form

$$U=\int_V U_0 dv=\frac{1}{2}\int_V \sigma_{ij}\varepsilon_{ij}dv+\frac{1}{2}\int_V \tau_{ij}\varepsilon_{ij}dv \tag{5}$$

In this relation, σ_{ij} and τ_{ij} are the normal and shear stresses, respectively. In addition, V is the volume of the beam. Based on the last equality, the following expression can be used for linear bending strain energy (Mohammadi *et al*. 2016)

$$U^b=\frac{1}{2}\int_0^L E_f(x) I_y \left(w''\right)^2 dx \tag{6}$$

in which w'' is the curvature of the beam. The moment of inertia about the y-axis I_y is formulated in the next shape (Yoo and Lee 2011)

$$I_y=\frac{t_f b_f^3}{6}\cos^3\alpha \tag{7}$$

In this equation, b_f and t_f define the flange width and thickness of I-section, respectively. The angle α is shown in Fig. 1. By inserting the Eqs. (2), (4) and (7) into relation (6), the lateral bending potential energy U^b can be obtained in the below form

$$U^b=\frac{1}{144}\frac{t_f b_f^3 w_k^2 k\pi\cos(\alpha)^3\left(2\pi^3k^3E_{f,L}+4\pi^3k^3E_{f,s}-3\pi kE_{f,L}+3\pi kE_{f,s}\right)}{L^3} \tag{8}$$

On the other hand, the torsional strain potential energy is found for two cases. The first one is the St. Venant's torsion, and the second one is warping. To obtain the general relation, the torsional stresses and strains are calculated explicitly and then, they are substituted in the Eq. (5). It should be added that the section of the beam is assumed to be open cross-section. Fig. 2 shows the lateral-torsional deformation pattern of beam having open cross-section.

It is reminded that the St. Venant's torsion moment M_x^{st} is expressed in the subsequent relation (Yoo and Lee 2011)

$$M_x^{st}=G_f(x)J(x)(\phi') \tag{9}$$

where ϕ' is the warping angle. Furthermore, the shear modulus and torsional constant are defined by G_f and J, respectively. Therefore, the St. Venant's torsion potential energy caused by free torsion of the beam can be written in the next form (Yoo and Lee 2011)

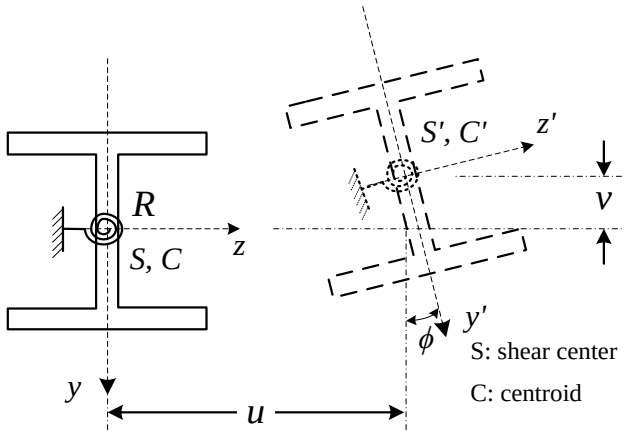

Fig. 2 The lateral-torsional deformation of beam section

$$U^{st}=\frac{1}{2}\int_0^L G_f(x)J(x)\left(\phi'\right)^2dx \tag{10}$$

Where, $G_f(x)$ is the function of shear modulus change along the structural length. Moreover, $J(x)$ is the torsional constant which is given by Yoo and Lee (2011)

$$J(x)=\frac{1}{3}\sum_{i=1}^{ne}b_i t_i^3 \tag{11}$$

in which *ne* is the number of I-shaped section elements. b_i and t_i are the width and thickness of each element of I-shape section. The resultant of relation $J(x)$ is obtained, as follows

$$J(x)=\frac{2}{3}b_f t_f^3\cos^3\alpha+\frac{2t_w^3\left(1-\frac{1}{2^{n+1}}\right)}{3(n+1)}h(x) \tag{12}$$

where n is the power constant in the function of elastic and shear modulus, which presents the change through the height of section. $h(x)$ is determined based on the Eq. (3). Also, t_w is the web thickness of I-section. The other geometric properties of section are demonstrated in Fig. 1. The relation of $J(x)$ is determined in Appendix. By substituting the relations Eqs. (2), (4) and (12) into the Eq. (10), the following St. Venant's torsional potential energy U^{st} can be developed.

$$\begin{aligned}U^{st}=\frac{1}{12}\frac{1}{k^2\pi^2L(n+1)}\Big(&\phi_k^2\Big(t_w^3\Big(\Big(\Big(\frac{1}{2}h_s-\frac{3}{2}h_L\Big)G_{f,L}+G_{f,s}h_L\Big)k^2\pi^2-\frac{1}{4}\Big(\Big(h_L\\&+\frac{1}{3}h_s\Big)G_{f,L}+\Big(h_L+\frac{5}{3}h_s\Big)G_{f,s}\Big)k^4\pi^4-\frac{1}{4}\left(\left(-3h_L+h_s\right)G_{f,L}+G_{f,s}\left(h_L\right.\right.\\&\left.\left.+h_s\right)\right)k^2\pi^2\Big)2^{-n}-2t_f^3k^2\pi^2b_f\left(-G_{f,L}+G_{f,s}\right)(n+1)\cos(\alpha)^3-2\Big(\Big(\Big(\frac{1}{2}h_s\\&-\frac{3}{2}h_L\Big)G_{f,L}+G_{f,s}h_L\Big)k^2\pi^2-\frac{3}{4}\left(-G_{f,L}+G_{f,s}\right)\left(h_L-h_s\right)\Big)t_w^3+\frac{4}{3}(n+1)k^2\\&t_f^3b_f\Big(k^2\Big(G_{f,s}+\frac{1}{2}G_{f,L}\Big)\pi^2+\frac{3}{4}G_{f,s}-\frac{3}{4}G_{f,L}\Big)\pi^2\cos(\alpha)^3+\frac{1}{2}\Big(\Big(\Big(h_L\\&+\frac{1}{3}h_s\Big)G_{f,L}+\Big(h_L+\frac{5}{3}h_s\Big)G_{f,s}\Big)k^4\pi^4+\left(\left(-3h_L+h_s\right)G_{f,L}+G_{f,s}\left(h_L+h_s\right)\right)k^2\pi^2\\&-3\left(-G_{f,L}+G_{f,s}\right)\left(h_L-h_s\right)\Big)t_w^3\Big)\Big)\end{aligned} \tag{13}$$

Another part of the linear strain energy is the related to the restrained torsion of the beam. To include this effect, the torsional potential energy U^w created by warping of the beam section is found, as follows (Yoo and Lee 2011)

$$\begin{aligned}U^w=&\frac{1}{2}\int_0^L E_f(x)I_w(x).\left(\phi''\right)^2dx\\&+\int_0^L E_f(x)I''_w(x)\left(\phi'\right)^2dx+\int_0^L E_f(x)I'_w(x)\left(\phi'\right)\left(\phi''\right)dx\end{aligned} \tag{14}$$

where the definition of I_w is as below (Yoo and Lee: 2011)

$$I_w(x)=\frac{I_y}{4}h(x)^2 \tag{15}$$

In the current equality, $h(x)$ is determined based on the Eq. (3). I_y has been also defined in Eq. (7). By employing Eqs. (2), (4) and (15) in Eq. (14), the limited torsional potential energy of the tapered beam can be rewritten in the succeeding form

$$\begin{aligned}U^w=&\frac{1}{720}\cdot\frac{1}{L^3}\Big(\phi_k^2\cos(\alpha)^3t_fb_f^3\Big(\Big(\Big(E_{f,s}+\frac{3}{2}E_{f,L}\Big)k^4\pi^4+\frac{95}{4}\Big(E_{f,s}+\frac{14}{19}E_{f,L}\Big)k^2\pi^2\\&-\frac{15}{4}E_{f,s}+\frac{15}{4}E_{f,L}\Big)h_L^2+\frac{7}{4}\Big(\Big(E_{f,s}+\frac{3}{7}E_{f,L}\Big)k^4\pi^4-\frac{205}{7}k^2\Big(E_{f,s}\\&+\frac{25}{41}E_{f,L}\Big)\pi^2+\frac{30}{7}E_{f,s}-\frac{30}{7}E_{f,L}\Big)h_sh_L+\frac{9}{4}\Big(\Big(E_{f,s}+\frac{1}{9}E_{f,L}\Big)k^4\pi^4\\&+\frac{125}{9}\Big(E_{f,s}+\frac{8}{25}E_{f,L}\Big)k^2\pi^2-\frac{5}{3}E_{f,s}+\frac{5}{3}E_{f,L}\Big)h_s^2\Big)\Big)\end{aligned} \tag{16}$$

3.2 Total energy of tapered beam

The lateral-torsional analysis of beam element can be performed by summation of lateral bending and St. Venant's torsional potential energy. It should be added that cross-section keeps the main shape after the buckling. According to the Fig. 3(a), the taper beam is under the concentrated moments and continues lateral bracing. In this figure, the lateral bracing is modeled by torsional spring through the beam length. The stiffness of torsional spring is defined by the coefficient R. On the other hand; the 3D combination of lateral and torsion deformations of cross-section is shown in Fig. 3(b).

By summation of Eqs. (6), (10) and (14), the elemental strain potential energy, in which the shear deformation and warping effect is ignored, can be expressed, as follows (Mohammadi *et al*. 2016)

$$\begin{aligned}U=&\frac{1}{2}\int_0^L E(x)I_y\left(w''\right)^2dx+\frac{1}{2}\int_0^L G(x)J(x)\left(\phi'\right)^2dx\\&+\frac{1}{2}\int_0^L E(x)I_w(x)\left(\phi''\right)^2dx+\int_0^L E(x)I_w^{*}(x)\left(\phi'\right)^2dx\\&+\int_0^L E(x)I_w^{'}(x)\left(\phi'\right)\left(\phi''\right)dx+\frac{1}{2}\int_0^L R\left(\phi\right)^2dx\end{aligned} \tag{17}$$

where the last term in Eq. (17) is the potential energy caused by the lateral bracing of the beam. R is the lateral bracing stiffness factor. There are two parallels coordinates for an open cross-section beam element. One of them is defined at the area center, and the other is stayed at the shear center. It should be added that the bending and torsional supports of the beam element are assumed to be simple. For this kind of the supports, the following boundary conditions should be considered

$$\begin{aligned}&w(0)=\phi(0)=w(L)=\phi(L)=0\\&w''(0)=\phi''(0)=w''(L)=\phi''(L)=0\end{aligned} \tag{18}$$

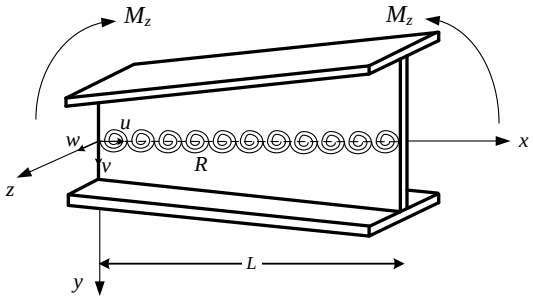

(a) The concentrated moments and continuum lateral bracing

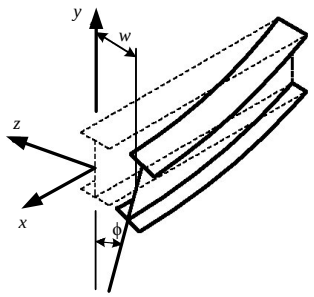

(b) The combination of lateral-torsional deformation model

Fig. 3 The model of tapered beam

Based on the Ritz method, the total potential energy of element was minimized. Due to variation of elastic modulus and cross-section properties along the length of the element, it was not easy to use variational principles for achieving the governing differential equation. Hence, by assuming trigonometric functions for the displacement's field and minimizing the total energy of element, the critical moment of element is obtained directly. On the other hand, the energy of external loading T can be calculated in the next shape (Yoo and Lee 2011)

$$T = -\frac{1}{2}\int_0^L 2Mw''\phi dx \tag{19}$$

It should be mentioned that the well-known total energy of element is obtained, as follows

$$\Pi = U + T \tag{20}$$

By inserting Eqs. (17) and (19) into relation (20), the succeeding total energy function can be developed

$$\begin{aligned}\Pi = {} & \frac{1}{144}\frac{t_f b_f^3 w_k^2 k\pi\cos(\alpha)^3\left(2\pi^3 k^3 E_{f,L}+4\pi^3 k^3 E_{f,s}-3\pi k E_{f,L}+3\pi k E_{f,s}\right)}{L^3} \\ & + \frac{1}{320}\frac{1}{L^3}\Big(\phi_k^2\Big(\Big(\frac{4}{9}\left(E_{f,s}+\frac{3}{2}E_{f,L}\right)k^4\pi^4+\frac{5}{3}k^2\left(E_{f,s}-2E_{f,L}\right)\pi^2-5E_{f,s} \\ & +5E_{f,L}\Big)h_L^2+\frac{7}{9}h_s\Big(\left(E_{f,s}+\frac{3}{7}E_{f,L}\right)k^4\pi^4+\frac{15}{7}k^2\left(E_{f,s}+E_{f,L}\right)\pi^2+\frac{90}{7}E_{f,s} \\ & -\frac{90}{7}E_{f,L}\Big)h_L+\Big(\left(E_{f,s}+\frac{1}{9}E_{f,L}\right)k^4\pi^4-\frac{5}{3}k^2\pi^2E_{f,s}-5E_{f,s}+5E_{f,L}\Big)h_s^2\Big)t_f \\ & b_f^3\cos(\alpha)^3\Big)+\frac{1}{12}\frac{1}{k^2\pi^2L(n+1)}\Big(\phi_k^2\Big(t_w^3\Big(\Big(\Big(\frac{1}{2}h_s-\frac{3}{2}h_L\Big)G_{f,L} \\ & +G_{f,s}h_L\Big)k^2\pi^2-\frac{1}{4}\Big(\Big(h_L+\frac{1}{3}h_s\Big)G_{f,L}+\Big(h_L+\frac{5}{3}h_s\Big)G_{f,s}\Big)k^4\pi^4-\frac{1}{4}\Big(\big(-3h_L \\ & +h_s\big)G_{f,L}+G_{f,s}\left(h_L+h_s\right)\Big)k^2\pi^2\Big)2^{-n}-2t_f^2k^2\pi^2b_f\left(-G_{f,L}+G_{f,s}\right)(n+1)\cos(\alpha)^3 \\ & -2\Big(\Big(\Big(\frac{1}{2}h_s-\frac{3}{2}h_L\Big)G_{f,L}+G_{f,s}h_L\Big)k^2\pi^2-\frac{3}{4}\left(-G_{f,L}+G_{f,s}\right)\left(h_L-h_s\right)\Big)t_w^3 \\ & +\frac{4}{3}(n+1)k^2t_f^3b_f\Big(k^2\Big(G_{f,s}+\frac{1}{2}G_{f,L}\Big)\pi^2+\frac{3}{4}G_{f,s}-\frac{3}{4}G_{f,L}\Big)\pi^2\cos(\alpha)^3 \\ & +\frac{1}{2}\Big(\Big(\Big(\Big(h_L+\frac{1}{3}h_s\Big)G_{f,L}+\Big(h_L+\frac{5}{3}h_s\Big)G_{f,s}\Big)k^4\pi^4+\big(\big(-3h_L+h_s\big)G_{f,L}+G_{f,s}\left(h_L\right. \\ & \left.+h_s\right)\big)k^2\pi^2-3\left(-G_{f,L}+G_{f,s}\right)\left(h_L-h_s\right)\Big)t_w^3\Big)\Big)+\frac{1}{2}\frac{Mw_kk^2\pi^2\phi_k}{L}+\frac{1}{4}R\phi_k^2L \\ & +\frac{1}{144}\frac{1}{k\pi L^3}\Big(\phi_k^2t_fb_f^3\cos(\alpha)^3\left(2\pi^3k^3E_{f,L}h_L^2-4\pi^3E_{f,L}h_Lh_s+2\pi^3k^3E_{f,L}h_s^2\right. \\ & +4\pi^3k^3E_{f,s}h_L^2-8\pi^3k^3E_{f,s}h_Lh_s+4\pi^3k^3E_{f,s}h_s^2+3\pi kE_{f,L}h_L^2-6\pi kE_{f,L}h_Lh_s \\ & \left.+3\pi kE_{f,L}h_s^2-3\pi kE_{f,s}h_L^2+6\pi kE_{f,s}h_Lh_s-3\pi kE_{f,s}h_s^2\right)\Big)-\frac{1}{96}\frac{1}{k\pi L^3}\Big(\\ & \phi_k^2\cos(\alpha)^3b_f^3t_f\Big(-2\pi^3k^3E_{f,L}h_L^2+2\pi^3k^3E_{f,L}h_Lh_s+2\pi^3k^3E_{f,s}h_Lh_s-2\pi^3k^3E_{f,s}h_s^2 \\ & +3\pi kE_{f,L}h_L^2-6\pi kE_{f,L}h_Lh_s+3\pi kE_{f,L}h_s^2-3\pi kE_{f,s}h_L^2+6\pi kE_{f,s}h_Lh_s-3\pi kE_{f,s} \\ & h_s^2\Big)\Big)\end{aligned} \tag{21}$$

To obtain the equilibrium, the derivatives of total energy function with respect to the general coordinates, w_k and ϕ_k, should be equal to zero. Therefore, the following relations are found

$$\frac{\partial\Pi}{\partial w_k}=0 \qquad \frac{\partial\Pi}{\partial\phi_k}=0 \tag{22}$$

where the factor of k can changes from 1 to m+2. By using the relation Eq. (22), the next system of equations can be established in the matrix form

$$\begin{bmatrix}\{C_{11}\} & \{C_{12}\}\\ \{C_{21}\} & \{C_{22}\}\end{bmatrix}\begin{Bmatrix}\{w_k\}\\ \{\phi_k\}\end{Bmatrix}=\begin{Bmatrix}\{0\}\\ \{0\}\end{Bmatrix} \tag{23}$$

It should be noted that once the relation of Eq. (23) is evaluated, it is required that the determinant of coefficients [C] be equal to zero ($|C| = 0$) with respect to the critical bending moment M. Based on this fact, the critical bending moment of tapered FG I-beam can be achieved in the below shape

$$\begin{aligned}M_{cr}= {} & -\frac{1}{3}\frac{1}{\pi 2^n(n+1)kL^2}\Big(\Big((n+1)b_f\Big(\frac{1}{2880}E_{f,L}^2\cos(\alpha)^3\pi^6k^6b_f^3h_s^2t_f(n \\ & +1)2^{n+1}+\Big(\frac{2}{9}(n+1)\Big(\frac{1}{40}k^6\Big(\Big(h_L^2+\frac{7}{4}h_Lh_s+\frac{9}{4}h_s^2\Big)E_{f,s}^2+2\Big(h_L^2+\frac{13}{16}h_Lh_s \\ & +\frac{11}{16}h_s^2\Big)E_{f,L}E_{f,s}+\frac{3}{4}\Big(h_L+\frac{1}{2}h_s\Big)h_LE_{f,L}^2\Big)b_f^2\pi^6+k^4\Big(\Big(\Big(-\frac{799}{640}h_Lh_s+\frac{527}{640}h_s^2 \\ & +\frac{49}{80}h_L^2\Big)E_{f,s}^2+\frac{119}{160}E_{f,L}\Big(h_L^2-\frac{461}{238}h_Lh_s+\frac{193}{238}h_s^2\Big)E_{f,s}+\frac{61}{320}E_{f,L}^2\Big(h_L^2 \\ & -\frac{259}{122}h_Lh_s+\frac{77}{122}h_s^2\Big)\Big)b_f^2+\Big(E_{f,s}+\frac{1}{2}E_{f,L}\Big)t_f^2\left(G_{f,L}+2G_{f,s}\right)L^2\Big)\pi^4 \\ & +\frac{9}{4}k^2\Big(\frac{5}{32}\Big(\Big(h_L^2-\frac{11}{5}h_Lh_s+\frac{7}{5}h_s^2\Big)E_{f,s}+\frac{4}{5}E_{f,L}\Big(h_L^2-\frac{7}{4}h_Lh_s+\frac{1}{2}h_s^2\Big)\Big)(\\ & -E_{f,L}+E_{f,s}\big)b_f^2+L^2t_f^2\left(-E_{f,L}G_{f,s}+E_{f,s}G_{f,L}\right)\Big)\pi^2+\frac{9}{8}\Big(-\frac{1}{16}\left(h_L-h_s\right)^2\left(-E_{f,L}\right. \\ & \left.+E_{f,s}\right)b_f^2+L^2t_f^2\left(G_{f,L}-G_{f,s}\right)\Big)\left(-E_{f,L}+E_{f,s}\right)\Big)b_ft_f\cos(\alpha)^3+\Big(k^2\Big(E_{f,s} \\ & +\frac{1}{2}E_{f,L}\Big)\pi^2+\frac{3}{4}E_{f,s}-\frac{3}{4}E_{f,L}\Big)\Big(\frac{1}{6}k^2t_w^3\Big(\left(G_{f,L}+G_{f,s}\right)h_L+\frac{1}{3}h_s\left(G_{f,L}\right. \\ & \left.+5G_{f,s}\right)\Big)\pi^2+R(n+1)L^2+\frac{1}{2}t_w^3\Big(h_L-\frac{1}{3}h_s\Big)\left(G_{f,L}-G_{f,s}\right)\Big)L^2\Big)2^n \\ & -\frac{1}{12}\Big(k^2\Big(E_{f,s}+\frac{1}{2}E_{f,L}\Big)\pi^2+\frac{3}{4}E_{f,s}-\frac{3}{4}E_{f,L}\Big)\Big(k^2\Big(\left(G_{f,L}+G_{f,s}\right)h_L \\ & +\frac{1}{3}h_s\left(G_{f,L}+5G_{f,s}\right)\Big)\pi^2+3\Big(h_L-\frac{1}{3}h_s\Big)\left(G_{f,L}-G_{f,s}\right)\Big)t_w^3L^2\Big)t_f\cos(\alpha)2^n\Big)^{1/2} \\ & \cos(\alpha)b_f\Big)\end{aligned} \tag{24}$$

The direction of this resultant moment is about *the* z-axis. So it can be the same as M_z. It is worth mentioning that effect of continuous lateral bracing of the tapered beam is defined by the factor of R. Based on this parameter, when the value of R tends to zero, the Eq. (24) expresses the relation of critical bending moment of the tapered I-beam without lateral bracing.

4. Numerical examples

In this section, to validate the proposed formulation, some numerical examples are analyzed. Then, the obtained results are compared with the others' answers. In addition, the effect of torsional stiffness and functionally graded material on the lateral-torsional buckling of the tapered beam is investigated, separately.

4.1 Prismatic I-shaped beam

To verify the proposed formulation, the lateral-torsional buckling of doubly-symmetrically prismatic I-beam without any lateral bracing is first studied. The concentrated moments are considered at the two ends of the beam. It should be added that the supports of the beam are simple. The model of I-beam is shown in Fig. 4. In 1943, the relation of buckling moment of prismatic I-beam was obtained by Schrader and Hill (1943). To apply the proposed formulation for the prismatic I-beam with homogenous section and without lateral bracing, the following values are utilized

$$\begin{aligned} &h_s = h_L = h && \text{Prismatic state} \\ &n = 0 && \text{Isotropic through height} \\ &\begin{cases} E_{f,s} = E_{f,L} = E \\ G_{f,s} = G_{f,L} = G \end{cases} && \text{Isotropic through length} \end{aligned} \tag{25}$$

By substituting the quantities of Eqs. (25) into (24), the critical moment of prismatic I-beam is achieved, as follows

$$M_{cr} = \frac{\pi\sqrt{EI_y\left(GJL^2 + I_w\pi^2 E\right)}}{L^2} \tag{26}$$

Based on this formula, it can be concluded that the proposed formulation can estimate the exact solution for the lateral-torsional buckling of homogenous I-beam. This solution clearly demonstrates the validation of the proposed scheme for the lateral-torsional analysis of prismatic I-beam (Schrader and Hill 1943).

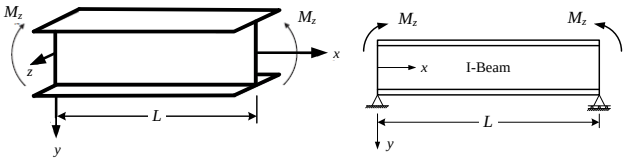

(a) Three-dimensional view (b) Two-dimensional view

Fig. 4 The model of I-shape beam with homogenous section

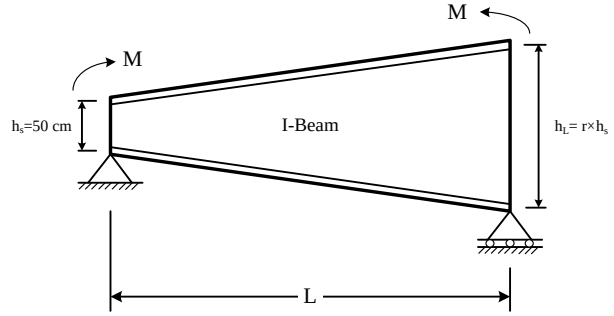

Fig. 5 The model of tapered I-shape beam with homogenous section

4.2 Tapered I-shaped beam

To show the generality of authors' formulation, a simply supported tapered I-beam is considered in this part. The beam element is under the effect of concentrated moment at the two ends. Fig. 5 demonstrates this model of the tapered I-beam.

It should be added that the lateral bracing of the beam is neglected. Therefore, the value of coefficient R is equal to zero. The height of cross-section changes linearly through the beam length. All sections of the beam are assumed to be homogenous, and the elastic modulus is equal to $E = 10^5$ MPa. Also, the Poisson's ratio is equal to 0.3. The cross-section height ratio at the end to the beginning of the beam is defined by r. This ratio is called *taper ratio*. Based on this, the following relation is existed for the angle of α

$$\cos(\alpha) = \frac{2L}{\sqrt{h_s^2(r-1)^2 + 4L^2}} \tag{27}$$

The height of cross-section at the start of the beam (h_s) is equal to 50 cm. In this case, the concentrated moments (M) are applied at the two ends of the beam. Furthermore, the geometric properties of beam section and the material characteristics are reported in Table 1.

For different values of the taper ratio and length, the beam critical moments are found and inserted in Table 2. As it is shown in this table, the results of first three modes of buckling are reported. To compare the outcomes, Figs. 6-8 are provided, as well. These figures show the changes of the beam critical moment versus taper ratio for different lengths. It should be noted that the Figs. 6-8 show the related results for three first modes of buckling, respectively.

It is obvious that the critical moment of beam increases by increasing the taper ratio. According to the results, the rate of critical moment growth decreases by increasing the taper ratio greater than 1.5. In other words, progression of the section height ratio at the end of the beam, more than 1.5 is not effective on the critical moment, significantly.

4.3 Continuously laterally supported prismatic I-shaped FG beam

At this stage, a simple supports prismatic FG I-beam

Table 1 The geometric properties of section at the start of the beam and mechanical characteristics of materials

Property	G (MPa)	E (MPa)	h_s (cm)	t_w (cm)	t_f (cm)	b_f (cm)
Value	$\frac{50000}{13}$	10^5	50.0	1.0	2.0	25.0

Table 2 The critical bending moment of tapered I-shape beam considering different taper ratio and beam length (*N.m*)

Taper ratio (r)	Buckling mode (k)	Length of beam (m)						
		20.0	15.0	10.0	8.0	4.0	2.0	1.0
0.1	1	8.882E+04	1.233E+05	2.041E+05	2.774E+05	8.363E+05	2.974E+06	1.093E+07
	2	1.901E+05	2.743E+05	4.898E+05	6.947E+05	2.374E+06	8.917E+06	3.332E+07
	3	3.138E+05	4.728E+05	9.024E+05	1.328E+06	4.829E+06	1.856E+07	6.977E+07
0.3	1	8.879E+04	1.227E+05	2.016E+05	2.723E+05	8.059E+05	2.851E+06	1.066E+07
	2	1.931E+05	2.800E+05	5.042E+05	7.214E+05	2.483E+06	9.413E+06	3.597E+07
	3	3.246E+05	4.943E+05	9.571E+05	1.418E+06	5.220E+06	2.024E+07	7.782E+07
0.5	1	8.918E+04	1.232E+05	2.019E+05	2.723E+05	8.028E+05	2.843E+06	1.080E+07
	2	1.976E+05	2.890E+05	5.278E+05	7.606E+05	2.661E+06	1.019E+07	3.963E+07
	3	3.390E+05	5.230E+05	1.030E+06	1.536E+06	5.729E+06	2.239E+07	8.759E+07
0.7	1	8.997E+04	1.245E+05	2.050E+05	2.775E+05	8.275E+05	2.957E+06	1.138E+07
	2	2.035E+05	3.010E+05	5.593E+05	8.131E+05	2.896E+06	1.118E+07	4.405E+07
	3	3.565E+05	5.577E+05	1.116E+06	1.677E+06	6.327E+06	2.488E+07	9.850E+07
0.9	1	9.116E+04	1.268E+05	2.110E+05	2.876E+05	8.778E+05	3.180E+06	1.236E+07
	2	2.108E+05	3.157E+05	5.975E+05	8.763E+05	3.174E+06	1.234E+07	4.897E+07
	3	3.767E+05	5.973E+05	1.214E+06	1.835E+06	6.992E+06	2.761E+07	1.100E+08
1.0	1	9.190E+04	1.282E+05	2.149E+05	2.944E+05	9.113E+05	3.326E+06	1.297E+07
	2	2.149E+05	3.239E+05	6.188E+05	9.113E+05	3.326E+06	1.297E+07	5.152E+07
	3	3.877E+05	6.188E+05	1.267E+06	1.919E+06	7.343E+06	2.903E+07	1.158E+08
1.5	1	9.694E+04	1.384E+05	2.427E+05	3.421E+05	1.139E+06	4.281E+06	1.657E+07
	2	2.392E+05	3.723E+05	7.411E+05	1.111E+06	4.173E+06	1.634E+07	6.398E+07
	3	4.497E+05	7.378E+05	1.553E+06	2.376E+06	9.220E+06	3.644E+07	1.430E+08
2.0	1	1.039E+05	1.527E+05	2.809E+05	4.062E+05	1.427E+06	5.406E+06	2.002E+07
	2	2.685E+05	4.296E+05	8.816E+05	1.336E+06	5.099E+06	1.982E+07	7.388E+07
	3	5.202E+05	8.704E+05	1.865E+06	2.870E+06	1.120E+07	4.380E+07	1.635E+08
3.0	1	1.224E+05	1.896E+05	3.746E+05	5.590E+05	2.059E+06	7.561E+06	2.359E+07
	2	3.369E+05	5.593E+05	1.189E+06	1.823E+06	6.998E+06	2.600E+07	8.139E+07
	3	6.755E+05	1.157E+06	2.525E+06	3.905E+06	1.517E+07	5.656E+07	1.772E+08

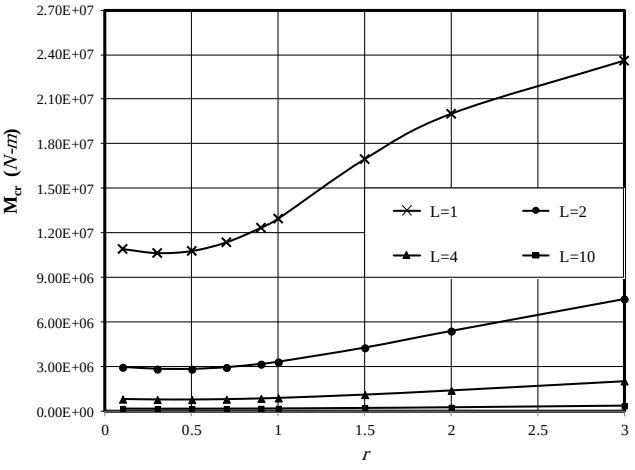

Fig. 6 The critical moment of first mode vs. taper ratio for various lengths of beam

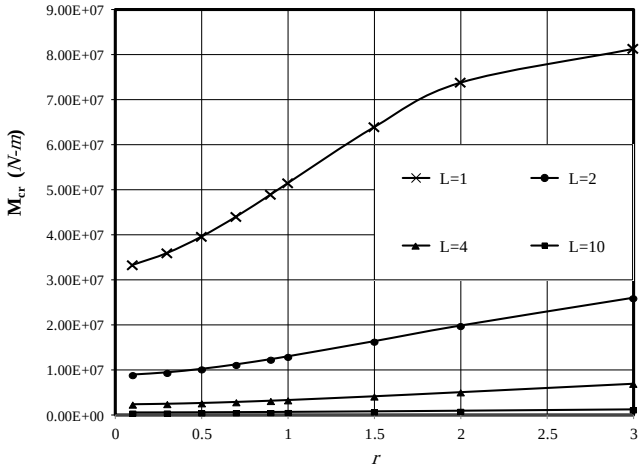

Fig. 7 The critical moment of second mode vs. taper ratio for various lengths of beam

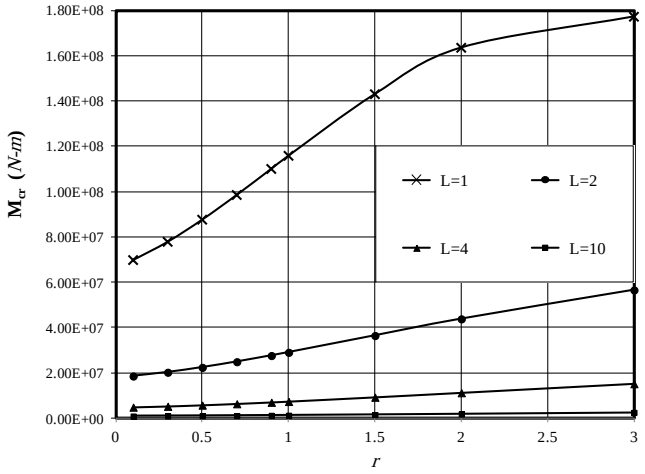

Fig. 8 The critical moment of third mode vs. taper ratio for various lengths of beam

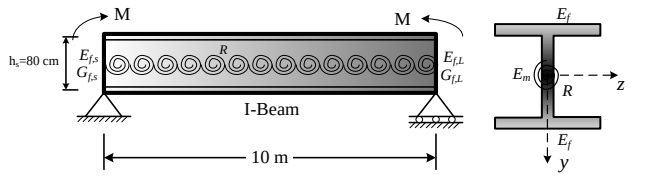

(a) Simply-supported beam with lateral bracing (b) Cross-section

Fig. 9 The model of simple supports I-beam considering functionally graded section

Table 3 The geometric properties of section and mechanical characteristics of materials

Characteristic	$G_{f,s}$ (MPa)	$E_{f,s}$ (MPa)	h_s (cm)	t_w (cm)	t_f (cm)	b_f (cm)
Value	$\frac{50000}{13}$	10^5	80.0	1.0	2.0	25.0

considering continuum lateral bracing is analyzed. The length of the beam in this example is assumed to be equal to 10 m. Fig. 9 shows this structure.

It should be added that the elastic and shear modulus change functionally graded along the height of section and length of the beam. The change of elastic and shear modulus follows up a power function. For this problem, the power constant of function is defined by n. On the other hand, the change of elastic and shear modulus is assumed to vary linearly through the beam length. According to prismatic beam geometry, the value of angle α is equal to zero. For this structure, the geometric properties of cross-section and the mechanical characteristics of material are provided in Table 3. It should be noted that a dimensionless coefficient, which called R_T, is defined for the lateral bracing stiffness (Masoodi and Moghaddam 2015, Shooshtari *et al*. 2015, Rezaiee-Pajand and Masoodi 2016). The relation of lateral bracing coefficient is as follows

$$R_T = \frac{1}{1+\frac{G_{f,s}J_s}{RL}} \qquad R = \frac{G_{f,s}J_s}{L}\left(\frac{R_T}{1-R_T}\right) \tag{28}$$

where $G_{f,s}$ and J_s are the shear modulus and torsional constant at the start section of the beam, respectively. It should be noted that the factor of β is used for the ratio of elastic modulus at the end to the beginning section of the beam. In other words, the elastic and shear modulus at the end of the beam are calculated as below.

$$E_{f,L} = \beta E_{f,s} \qquad G_{f,L} = \beta G_{f,s} \tag{29}$$

The results of critical moment are reported in Tables 4 and 5 for different cases of the factors β and n. All values of the dimensionless coefficient of R_T are given in these tables. To compare the outputs of analysis, the changes of the beam critical moment versus the power constant and ratio of elastic modulus for different values of R_T are shown in Figs. 10 and 11, respectively. The relation of lateral bracing

Table 4 The critical bending moment of I-beam for different power constants and lateral bracing stiffness (β = 1.0) ($N.m$)

Power constant (n)	Buckling mode (k)	Dimensionless coefficient (R_T)				
		0.8	0.6	0.4	0.2	0.0
0.0	1	4.496E+05	3.493E+05	3.087E+05	2.862E+05	2.719E+05
	2	9.650E+05	9.225E+05	9.079E+05	9.006E+05	8.961E+05
	3	1.959E+06	1.938E+06	1.931E+06	1.928E+06	1.926E+06
1.0	1	4.421E+05	3.445E+05	3.051E+05	2.833E+05	2.694E+05
	2	9.595E+05	9.186E+05	9.045E+05	8.974E+05	8.931E+05
	3	1.955E+06	1.935E+06	1.928E+06	1.925E+06	1.923E+06
2.0	1	4.371E+05	3.413E+05	3.027E+05	2.814E+05	2.678E+05
	2	9.558E+05	9.159E+05	9.023E+05	8.954E+05	8.912E+05
	3	1.952E+06	1.932E+06	1.926E+06	1.923E+06	1.921E+06
3.0	1	4.335E+05	3.390E+05	3.010E+05	2.800E+05	2.667E+05
	2	9.532E+05	9.141E+05	9.007E+05	8.939E+05	8.898E+05
	3	1.950E+06	1.931E+06	1.924E+06	1.921E+06	1.919E+06

Table 5 The critical bending moment of I-beam for different ration of elastic modulus and lateral bracing stiffness (n = 0.0) ($N.m$)

Coefficient (β)	Buckling mode (k)	Dimensionless coefficient (R_T)				
		0.8	0.6	0.4	0.2	0.0
1.0	1	4.496E+05	3.493E+05	3.087E+05	2.862E+05	2.719E+05
	2	9.650E+05	9.225E+05	9.079E+05	9.006E+05	8.961E+05
	3	1.959E+06	1.938E+06	1.931E+06	1.928E+06	1.926E+06
2.0	1	5.387E+05	4.329E+05	3.913E+05	3.688E+05	3.546E+05
	2	1.255E+06	1.212E+06	1.197E+06	1.190E+06	1.185E+06
	3	2.591E+06	2.570E+06	2.563E+06	2.560E+06	2.558E+06
3.0	1	6.260E+05	5.161E+05	4.739E+05	4.513E+05	4.372E+05
	2	1.544E+06	1.501E+06	1.486E+06	1.479E+06	1.474E+06
	3	3.223E+06	3.202E+06	3.195E+06	3.192E+06	3.190E+06
4.0	1	7.121E+05	5.992E+05	5.565E+05	5.339E+05	5.198E+05
	2	1.833E+06	1.790E+06	1.775E+06	1.768E+06	1.763E+06
	3	3.855E+06	3.834E+06	3.827E+06	3.824E+06	3.822E+06

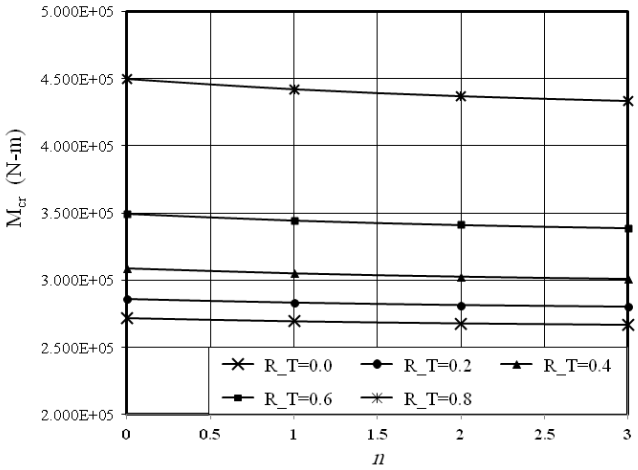

Fig. 10 The critical moment of first mode vs. power constant for different stiffness of lateral bracing

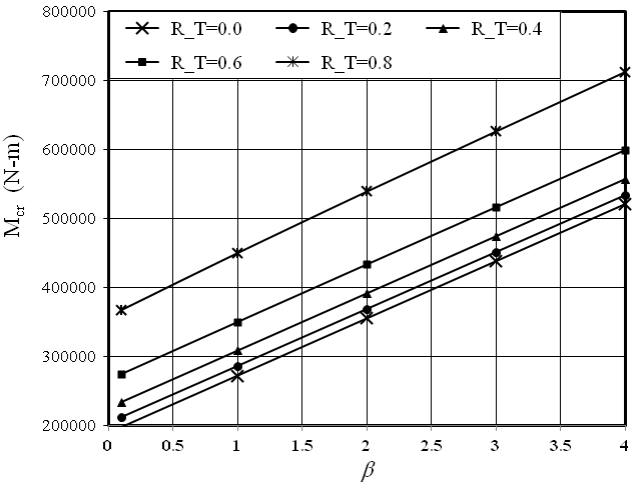

Fig. 11 The critical moment of first mode vs. ratio of elastic modulus for different stiffness of lateral bracing

stiffness considering the effect of power constant on the torsional constant is obtained, as follows

$$R = -\frac{5128.205127\left(-0.40+(1.00\,n+1.40)\,2^{n+1}\right)R_T}{2^{n+1}\,(n+1)\left(R_T-1\right)} \tag{30}$$

It is harvested that the variation of critical moment, caused by lateral bracing stiffness, is more noticeable for the first mode compared to the others. In other words, the effect of lateral bracing stiffness on the critical moment is not significant for the third mode of buckling. According to Fig. 11, the critical moment changes versus the factor β follow a linear pattern. Therefore, by growing up the factor β, the critical moment of the beam is increased.

5. Conclusions

In this study, the lateral-torsional analysis of doubly-symmetrically tapered I-beam is performed. The beam section is made of functionally graded material. The power functions are considered for the variation of elastic and shear modulus through the height of section and beam length. Based on the St. Venant's torsional and Euler-Bernoulli bending theories, the total energy of tapered I-beam under the effects of concentrated moments is formulated. By minimizing the total potential energy, the governing equation of beam element is obtained. The effect of continuous lateral bracing of the beam on the critical moment is investigated. To validate the Author's scheme, some practical numerical examples are solved. By comparing the obtained results with the other available ones, the accuracy and correctness of the present formulation are revealed. Furthermore, parametric studies conclude the following points:

(1) By increasing the length of the beam, the effect of taper ratio on the critical moment is decreased. In

other words, for the beam element with more than 10 m length, the growth of taper ratio up to the value 3 is not significantly effective.

(2) The critical moment of the beam is increased by raising the value of taper ratio. It should be added, the rate of critical moment increasing is reduced when the taper ratio of the beam grows up more than 3.

(3) By increasing the ratio of elastic modulus along the beam length, the structural critical moment is raised. For the different values of lateral bracing stiffness, the rate of critical moment increasing via the growing of the elastic modulus ratio is constant. Therefore, the lateral bracing stiffness is not effective on the rate of critical moment increasing via the growing the ratio of elastic modulus.

(4) According to Fig. 10, when the power constant of elastic and shear modulus variation function is increased, the critical moment of beam element is decreased. It is noted that the pattern of variation of elastic and shear modulus along the height of section is assumed to be symmetrical.

(5) By increasing the stiffness of lateral bracing of the beam, the effect of power constant on the variation of critical moment is amplified. In other words, the rate of critical moment decreasing via the growing the value of power constant is more for the high values of lateral bracing stiffness.

Based on the results of Tables 4 and 5, it is obvious that the effect of lateral bracing stiffness increasing on the critical moment of first mode is more than that of the other modes. On the other hand, the effect of lateral bracing stiffness on the critical moment is not significant for the third mode of buckling.

Funding

This research did not receive any specific grant from funding agencies in the public, commercial, or not-for-profit sectors.

Conflict of interest

The authors declare that they have no conflict of interest.

References

Andrade, A. and Camotim, D. (2004), "Lateral-torsional buckling of prismatic and tapered thin-walled open beams: assessing the influence of pre-buckling deflections", *Steel Compos. Struct., Int. J.*, **4**(4), 281-301.

Attard, M.M. and Kim, M.-Y. (2010), "Lateral buckling of beams with shear deformations–A hyperelastic formulation", *Int. J. Solids Struct.*, **47**(20), 2825-2840.

Aydin, R., Gunaydin, A. and Kirac, N. (2015), "On the evaluation of critical lateral buckling loads of prismatic steel beams", *Steel Compos. Struct., Int. J.*, **18**(3), 603-621.

Banerjee, J.R. and Fisher, S.A. (1992), "Coupled bending-torsional dynamic stiffness matrix for axially loaded beam elements", *Int. J. Numer. Methods Eng.*, **33**(4), 739-751.

Banerjee, J.R. and Williamsm F.W. (1994), "Coupled bending-torsional dynamic stiffness matrix of an axially loaded timoshenko beam element", *Int. J. Solids Struct.*, **31**(6), 749-762.

Barretta, R., Feo, L. and Luciano, R. (2015), "Some closed-form solutions of functionally graded beams undergoing nonuniform torsion", *Compos. Struct.*, **123**, 132-136.

Bokaian, A. (1988), "Natural frequencies of beams under compressive axial loads", *J. Sound Vib.*, **126**(1), 46-65.

Bokaian, A. (1990), "Natural frequencies of beams under tensile axial loads", *J. Sound Vib.*, **142**(3), 481-498.

El-Mahdy, G.M. and El-Saadawy, M.M. (2015), "Ultimate strength of singly symmetric I-section steel beam with variable flange ratio", *Thin-Wall. Struct.*, **87**, 149-157.

Fatmi, R.E. (2007), "Non-uniform Warping Including the Effects of Torsion and Shear Forces. Part I: A General Beam Theory", *Int. J. Solids Struct.*, **44**, 5912-5929.

Gellert, M. and Gluck, J. (1972), "The influence of axial load on eigen-frequencies of a vibrating lateral restraint cantilever", *Int. J. Mech. Sci.*, **14**(11), 723-728.

Gupta, L.M., Ronghe, G.N. and Naghate, M.K. (2003), "Behaviour and stability of prestressed steel plate girder for torsional buckling", *Steel Compos. Struct., Int. J.*, **3**(1), 65-73.

Hashemi, S.M. and Richard, M.J. (2000a), "A Dynamic Finite Element (DFE) method for free vibrations of bending-torsion coupled beams", *Aerosp. Sci. Technol.*, **4**(1), 41-55.

Hashemi, S.M. and Richard, M.J. (2000b), "Free vibrational analysis of axially loaded bending-torsion coupled beams: a dynamic finite element", *Comput. Struct.*, **77**(6), 711-724.

Hashemi, S.M., Richard, M.J. and Dhatt, G. (1999), "A new Dynamic Finite Element (DFE) formulation for lateral free vibrations of Euler-Bernoulli spinning beams using trigonometric shape functions", *J. Sound Vib.*, **220**(4), 601-624.

Huang, Y. and Li, X.F. (2011), "Buckling Analysis of Nonuniform and Axially Graded Columns with Varying Flexural Rigidity", *J. Eng. Mech.*, **137**(1), 73-81.

Ioannidis, G.I. and Avraam, T.P. (2012), "Lateral-torsional buckling of simply supported beams under uniform bending and axial tensile force", *Arch. Appl. Mech.*, **82**(10), 1393-1402.

Ioannidis, G., Mahrenholtz, O. and Kounadis, A.N. (1993), "Lateral post-buckling analysis of beams", *Arch. Appl. Mech.*, **63**(3), 151-158.

Joshi, A. and Suryanarayan, S. (1984), "Coupled flexural-torsional vibration of beams in the presence of static axial loads and end moments", *J. Sound Vib.*, **92**(4), 583-589.

Joshi, A. and Suryanarayan, S. (1989), "Unified analytical solution for various boundary conditions for the coupled flexural-torsional vibration of beams subjected to axial loads and end moments", *Int. J. Solids Struct.*, **20**(2), 167-178.

Joshi, A. and Suryanarayan, S. (1991), "Iterative method for coupled flexural-torsional vibration of initially stressed beams", *J. Sound Vib.*, **146**(1), 81-92.

Jun, L., Rongying, S., Hongxing, H. and Xianding, J. (2004), "Coupled bending and torsional vibration of axially loaded Bernoulli-Euler beams including warping effects", *Appl. Acoust.*, **65**(2), 153-170.

Khelil, A. and Larue, B. (2008), "Simple Solution for the flexural-torsional buckling of laterally restrained I-beams", *Eng. Struct.*, **30**(10), 2923-2934.

Kim, N.-I. and Lee, J. (2014), "Exact solutions for stability and free vibration of thin-walled Timoshenko laminated beams under variable forces", *Arch. Appl. Mech.*, **84**(12), 1785-1809.

Kim, N.-I., Jeon, C.-K. and Lee, J. (2013), "Dynamic stability analysis of shear-flexible composite beams", *Arch. Appl. Mech.*, **83**(5), 685-707.

Kuś, J. (2015), "Lateral-torsional buckling steel beams with simultaneously tapered flanges and web", *Steel Compos. Struct.*, *Int. J.*, **19**(4), 897-916.

Lanc, D., Turkalj, G., Vo, T.P. and Brnić, J. (2016), "Nonlinear buckling behaviours of thin-walled functionally graded open section beams", *Compos. Struct.*, **152**, 829-839.

Larue, B., Khelil, A. and Gueury, M. (2007), "Elastic flexural–torsional buckling of steel beams with rigid and continuous lateral restraints", *J. Constr. Steel Res.*, **63**(5), 692-708.

Lee, S.-H., Kim, Y.-H. and Choi, S.-M. (2015), "Ultimate strength of long-span buildings with P.E.B (Pre-Engineered Building) system", *Steel Compos. Struct., Int. J.* **19**(6), 1483-1499.

Leung, A.Y.T. (1991), "Natural shape functions of a compressed Vlasov element", *Thin-Wall. Struct.*, **11**(5), 431-438.

Li, S.R. and Batra, R.C. (2013), "Relations between buckling loads of functionally graded Timoshenko and homogeneous Euler–Bernoulli beams", *J. Compos. Struct.*, **95**, 5-9.

Masoodi, A.R. and Moghaddam, S.H. (2015), "Nonlinear dynamic analysis and natural frequencies of gabled frame having flexible restraints and connections", *KSCE J. Civil Eng.*, **19**(6), 1819-1824.

Michaltsos, G.T. and Raftoyiannis, I.G. (2012), "The influence of prestressing on the twisting phenomenon of beams", *Arch. Appl. Mech.*, **82**(10), 1531-1540.

Mohammadi, E., Hosseini, S.S. and Rohanimanesh, M.S. (2016), "Elastic lateral-torsional buckling strength and torsional bracing stiffness requirement for mono-symmetric I-beams", *Thin-Wall. Struct.*, **104**, 116-125.

Murthy, M. and Neogy, J. (1969), "Determination of fundamental natural frequencies of axially loaded columns and frames", *J. Inst. Engt.* (*India*) *Civil Eng. Div.*, **49**, 201-212.

Nguyen, C.T., Moon, J., Le, V.N. and Lee, H.-E. (2010), "Lateral-torsional buckling of I-girders with discrete torsional bracings", *J. Constr. Steel Res.*, **66**(2), 170-177.

Nguyen, C.T., Joo, H.S., Moon, J. and Lee, H.E. (2012), "Flexural-torsional buckling strength of I-girders with discrete torsional bracing under various load conditions", *Eng. Struct.*, **36**, 337-350.

Nguyen, X.-H., Kim, N.-I. and Lee, J. (2015), "Optimum design of thin-walled composite beams for flexural–torsional buckling problem", *Compos. Struct.*, **132**, 1065-1074.

Nguyen, H.X., Lee, J., Vo, T.P. and Lanc, D. (2016), "Vibration and lateral buckling optimisation of thin-walled laminated composite channel-section beams", *Compos. Struct.*, **143**, 84-92.

Nishino, F., Kasemset, C. and Lee, S.L. (1973), "Variational formulation of stability problems for thin-walled members", *Ingenieur-Archiv*, **43**(1), 58-68.

Orloske, K. and Parker, R.G. (2006), "Flexural-torsional buckling of misaligned axially moving beams: II. Vibration and stability analysis", *Int. J. Solids Struct.*, **43**(14-15), 4323-4341.

Pavlović, R. and Kozić, P. (2003), "Almost sure stability of the thinwalled beam subjected to end moments", *Theor. Appl. Mech.*, **30**(3), 193-207.

Pavlović, R., Kozić, P., Rajković, P. and Pavlović, I. (2007), "Dynamic stability of a thin-walled beam subjected to axial loads and end moments", *J. Sound Vib.*, **301**(3-5), 690-700.

Pi, Y.L. and Bradford, M.A. (2002), "Elastic flexural-torsional buckling of continuously restrained arches", *Int. J. Solids Struct.*, **39**(8), 2299-2322.

Rezaiee-Pajand, M. and Masoodi, A.R. (2016), "Exact natural frequencies and buckling load of functionally graded material tapered beam-columns considering semi-rigid connections", *J. Vib. Control*, **24**(9), 1787-1808.

Sankar, B.V. (2001), "An elasticity solution for functionally graded beams", *Compos. Sci. Technol.*, **61**(5), 689-696.

Schrader, R.K. and Hill, H.N. (1943), "Lateral stability of unsymmetrical I-beams and trusses in bending", *Transact. Am. Soc. Civil Engr.*, **108**(1), 261-265.

Schurig, M. and Bertram, A. (2011), "The torsional buckling of a cruciform column under compressive load with a vertex plasticity model", *Int. J. Solids Struct.*, **48**(1), 1-11.

Shooshtari, A., Heyrani Moghaddam, S. and Masoodi, A. (2015), "Pushover analysis of gabled frames with semi-rigid connections", *Steel Compos. Struct., Int. J.*, **18**(6), 1557-1568.

Taylor, A.C. and Ojalvo, M. (1966), "Torsional restraint of lateral buckling", *J. Struct. Div. ASCE*, **92**(ST2), 115-129.

Tsai, H.-C. and Kelly, J.M. (2005), "Buckling of short beams with warping effect included", *Int. J. Solids Struct.*, **42**, 239-253.

Valentino, J. and Trahair, N.S. (1998), "Torsional restraint against elastic lateral buckling", *J. Struct. Eng. ASCE*, **124**(10), 1217-1226.

Vieira, R.F., Lisi, D. and Virtuoso, F.B. (2014), "Dynamic analysis of bridge girders submitted to an eccentric moving load", *Struct. Eng. Mech., Int. J.*, **52**(1), 173-203.

Vo, T.P., Lee, J., Lee, K. and Ahn, N. (2011), "Vibration analysis of thin-walled composite beams with I-shaped cross-sections", *Compos. Struct.*, **93**(2), 812-820.

Winter, G. (1958), "Lateral bracing of columns and beams", *J. Struct. Div. ASCE*, **84**(2), 1561-1583.

Ying, J., Lu, C.F. and Chen, W.Q. (2008), "Two-dimensional elasticity solutions for functionally graded beams resting on elastic foundations", *J. Compos. Struct.*, **84**(3), 209-219.

Yoo, C.H. and Lee, S. (2011), *Stability of Structures*: *Principles and Applications*, Elsevier.

Yoon, K. and Lee, P.-S. (2014), "Modeling the warping displacements for discontinuously varying arbitrary cross-section beams", *Compos. Struct.*, **131**, 56-69.

BU

Appendix

To obtain the relation of $J(x)$, the following procedure can be used. First of all, when a web-tapered I-beam twists about the x axis with a twisting angle ϕ, the twisting angle of top flange ϕ_f about is found below.

$$\phi_f = \phi \cos\alpha \tag{31}$$

The resultant free torsional torque of top flange is given by

$$T_f = GJ_f \phi' \cos^2\alpha \tag{32}$$

where J_f is defined by the following expression.

$$J_f = \frac{b_f t_f^3}{3} \tag{33}$$

Due to symmetric distribution of elastic modulus through the height of cross-section, the torque of section caused by free torsional deformation is found as follow.

$$T = 2T_f \cos\alpha + T_w = G_f(x) J(x) \phi' \tag{34}$$

where T_w defines the free torsional torque of web. The formulation of this factor is given by.

$$T_w = \int_{-\frac{h}{2}}^{\frac{h}{2}} \int_{-\frac{t_w}{2}}^{\frac{t_w}{2}} 4G(y) \phi' z^2 dz dy \tag{35}$$

By substituting the relation (1) into equation (35), the following expression is released.

$$T_w = G_f(x) \phi' \frac{2t_w^3 \left(1 - \frac{1}{2^{n+1}}\right)}{3(n+1)} h(x) \tag{36}$$

By using relations (34) and (36), the equivalent free torsional constant of section $J(x)$ is obtained in Eq. (12).